

Hydrophobic Hybrid Inorganic–Organic Thin Film Prepared by Sol–Gel Process for Glass Protection and Strengthening Applications

AMIR ERSHAD–LANGROUDI, CHRISTIAN MAI, GERARD VIGIER, RENE VASSOILLE

Laboratoire G.E.M.P.P.M. u.m.r., CNRS 5510-INSA, 69621 Villeurbanne, France

Received 19 July 1996; accepted 16 October 1996

ABSTRACT: Hybrid systems based on 3-trimethoxysilyl propyl methacrylate, tetramethylorthosilicate, and methyl methacrylate were developed for moisture protection and strengthening of glass objects. The hydrophobic behavior of the hybrid was obtained by adding different fluorinated precursors to the hybrid solution. Experimental results show that among different fluorinated precursors, 1H,1H,2H,2H-perfluorooctyl trichlorosilane gives the best results, increasing the water contact angle up to 100° and decreasing the free surface energy. Coated glasses exhibit higher strength (more than 50%) than uncoated glasses. The strengthening was interpreted in terms of a healing mechanism. © 1997 John Wiley & Sons, Inc. *J Appl Polym Sci* **65**: 2387–2393, 1997

Key words: hybrid material; sol–gel; hydrophobic surface; coating; thin film; strengthening of glass

INTRODUCTION

Glass is a material with excellent properties such as high chemical resistance and high transparency.^{1,2} However, some glasses can be sensitive to moisture and surface flaws. Thus it should be interesting to protect these glasses with a coating.

For these applications the qualities of a coating are mainly the following: good adhesion, the presence of a hydrophobic surface, and improvement of mechanical properties.

Pure organic and inorganic coatings have been used. Polymer coatings lead to good adhesion but do not really improve the mechanical properties. Inorganic coatings often have poor adhesion, especially for thicknesses higher than 1 μm .^{3,4}

Hybrid organic–inorganic coatings may combine the qualities of both materials, and they have

always been used for protection and strengthening of glass as shown by the recent promising works of Schmidt et al.^{5–11} Furthermore, hydrophobic surface modification based on perfluorosilane can be obtained.^{12,13}

The aim of this work was to study the influence of a hybrid coating film with the following characteristics: hydrophobicity, adhesion, and strengthening of glass objects.

EXPERIMENTAL

Materials

3-Trimethoxysilyl propyl methacrylate (TMSM), tetramethylorthosilicate (TMOS), methyl methacrylate (MMA), 1H,1H,2H,2H-perfluorooctyl trichlorosilane (FOTCS), 1H,1H,2H,2H-perfluorododecan-1-ol (FD1OL), 2,2,2-trifluoroethyl methacrylate (TFEM), and 1H,1H,2H-perfluoro-1-dodecene (F1D) from Aldrich were used without further purification. Formamid ethylene glycol

Correspondence to: Dr. A. Ershad–Langroudi.

Journal of Applied Polymer Science, Vol. 65, 2387–2393 (1997)

© 1997 John Wiley & Sons, Inc.

CCC 0021-8995/97/122387-07

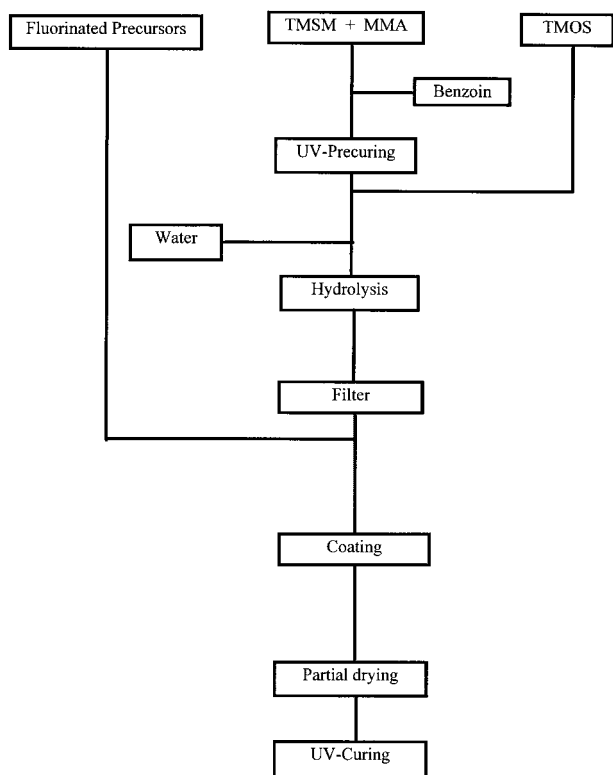


Figure 1 Synthesis schema developed for the hybrid system.

and heptane (reagent grades) were used as received.

Processing

A UV precuring system was synthesized by adding 2 wt % of a photoinitiator (benzoine) to TMSM and MMA. And then TMOS with different ratios of TMSM/TMOS were added to the TMSM/MMA system. Hydrolysis and condensation of TMSM and TMOS occur by slowly adding the substoichiometric amount of water (pH 2.5) to this formulation while stirring. Then the solution was stirred for 1 h at room temperature. Finally the solution was filtered through a 1- μ m filter. To achieve hydrophobic surfaces, different concentrations of the fluorinated precursors (FOTCS, F1D, FD1OL, TFEM) were added to the system, followed by stirring for 30 min.

Coating films with different thicknesses can be prepared as a function of time and viscosity. Coating experiments were carried out by a dip coating technique with thin soda lime glass slides used as substrates. The substrate was immersed in a

dipping solution and was drawn up vertically. The films were dried at room temperature before UV curing. The developed synthesis schema is summarized in Figure 1.

Techniques

Contact Angle Measurements

The advancing contact angles of the coatings were measured at room temperature. A Hamilton microliter syringe was used to place a drop of liquid onto a coating plate. Advancing angles were measured by a Ramé Hart's goniometer. The surfaces were cleaned with ethanol and distilled/deionized water before each experiment.

Adhesion Test

A qualitative adhesion test was used on the coating film.¹⁴ First, a coated sample was precleaned with ethanol. Next, a sharp razor was used to prepare a net of cuts in the sample. The cuts were spaced 1 mm apart and 11 such cuts were made in both orthogonal directions. Then the films were lightly brushed with soft tissue to remove any detached flakes. A pressure-sensitive adhesive tape was then uniformly applied to the clean surface. After 1 min of application, the tape was removed by pulling it off as close to an 180° angle as possible. Following peel, the grid area was inspected for removal of the coating from the substrate. The hybrid-glass interface was observed by scanning electron microscopy (SEM).

Table I Mean Values of Contact Angles of Water for Different Coating Compositions in TMSM-TMOS-MMA (1 : 1 : 0.5) System

Composition	Advance Contact Angles (θ°)
Uncoated glass	10 \pm 5
Coated glass without fluorinated precursors	49 \pm 5
+ TFEM 2 wt %	61 \pm 4
+ TFEM 8 wt %	65 \pm 6
+ TFEM 30 wt %	66 \pm 4
+ F1D 2 wt %	60 \pm 5
+ FD1O1 2 wt %	70 \pm 3
+ FD1OL 3 wt %	85 \pm 5
+ FOTCS 3 wt %	100 \pm 5

Table II Surface Free Energies (mJ/m²) of Liquid Used for Contact Angle Measurements

Liquid	γ_1	γ_1^d	γ_1^p
Water	72.8	21.8	51.0
Formamide	58.2	39.4	18.7
Ethylene glycol	48.3	29.3	19.3
Heptane	20.3	20.3	0

Adapted from Marconi et al.³⁰

Biaxial Flexion Test

A biaxial flexion test was used to determine the rupture strength.¹⁵ Six kinds of samples (microscope slides $40 \times 40 \times 2 \text{ mm}^3$) were used in this test:

1. raw samples (as received);
2. abrasive samples (polished with 320 grain emery cloth normalized by application 800 g load during 30 s) before coating;
3. indented samples (10 N load during 10 s with a Wolpert microindenter) before coating; and
- 4–6. samples 1–3 with a coating.

RESULTS AND DISCUSSION

All the final coatings displayed optical transparency that indicated that the metal alkoxides were well mixed with the organic precursors, showing that no macrophase separation occurred. Indeed, the preparation methods of these coating systems were similar to those used in our early studies.^{16–18} Crack free transparent coatings on glass of about $15 \mu\text{m}$ were obtained after UV curing all compositions (see Table I).

Hydrophobic Behavior

We already observed that the contact angle for unfluorinated base hybrid increased up to 50° in

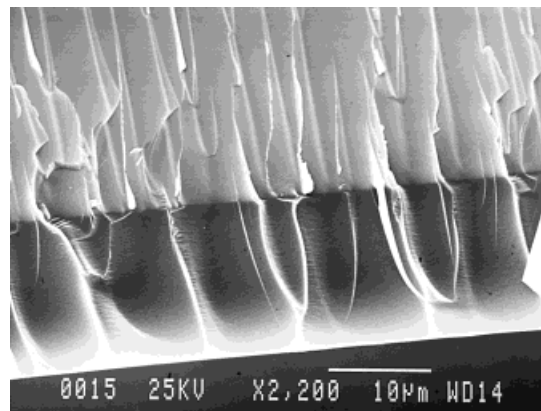


Figure 2 SEM of the hybrid-glass interface. The thickness of the coating is about $15 \mu\text{m}$.

comparison with uncoated glass (10°). For increasing the hydrophobic properties, different fluorinated precursors were added to the system (see Table I).

The fluorine groups TFEM and F1D have $-\text{CH}=\text{CH}_2$ bonds. They can be dissolved physically in a hybrid solution before UV curing. Adding different amounts of TFEM to the base hybrid induced only a small increase in the contact angle for water, even for a high concentration of TFEM (30 wt %). The same results were obtained with F1D containing a $\text{C}_{10}\text{F}_{21}$ fluorinated chain. This may be due to the fact that these fluorine groups (TFEM, F1D) had not reacted with other components in the hybrid solution. Therefore, during the dip coating process, most of the fluorinated chain could be eliminated from the surface of coated glass.

The addition of the FD1OL, containing a $\text{C}_{10}\text{F}_{21}$ fluorinated chain, had a remarkable influence on the wetting behavior. This hydrophobic coating led to a water contact angle of $50\text{--}85^\circ$, depending on the FD1OL content. One possible explanation is that the OH group in this fluorine chain can react with the other components (TMSM, TMOS).

Table III Polar (γ_s^p), Dispersive (γ_s^d), and Total (γ_s) Surface Tension of Coating Systems and Their Polarity Parameter (X_p) with PTFE and Glass for Comparison

Composition	γ_s (mJ/m ²)	γ_s^p (mJ/m ²)	γ_s^d (mJ/m ²)	X_p
TMSM : TMOS : MMA				
Glass	68.2	50.7	17.5	0.74
1 : 1 : 0.5	46.8	26.3	20.5	0.56
1 : 1 : 0.5 + 3% FOTCS	23.6	4.5	19.1	0.24
PTFE	20.2	2.23	17.9	0.11

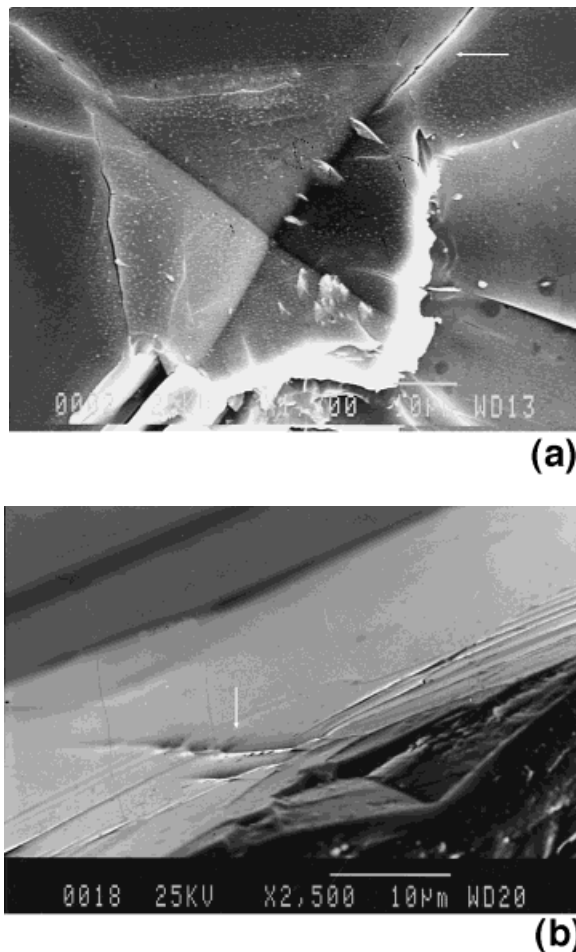


Figure 3 SEM of the indented samples: (a) without coating and (b) with coating; the arrows show the filled crack before and after coating.

But the best results were obtained with the FOTCS precursors. Adding only 3 wt % FOTCS led to a water contact angle reaching 100°. This effect could be attributed to the SiCl_3 bonds of fluorinated chains with silane groups of the hybrid network, inducing an easy insertion of fluorinated groups. This insertion led to the presence of fluorinated chains at the air interface, which was responsible for the influence on the wetting behavior.¹⁹ In fact, it is known from Langmuir-Blodgett model that only the outermost part of the surface determines the wetting properties.²⁰ In consideration of the good results obtained with FOTCS precursors, the following work was focused on the TMSM-TMOS-MMA/FOTCS system. To get more information on the surface energy of the hydrophobic coating, the contact angle measurements were carried out by using probe

liquids (Table II) other than water.^{21–30} To determine the polar (γ_S^p) and dispersive (γ_S^d) components of the surface tension, we used the Young equation, eq. (1),

$$\begin{aligned} \gamma_1(1 + \cos \theta)/2(\gamma_1^d)^{0.5} \\ = (\gamma_S^d)^{0.5} + (\gamma_S^p)^{0.5} * (\gamma_1^p/\gamma_1^d)^{0.5} \quad (1) \end{aligned}$$

where θ is the measured value of the advancing contact angle and γ_1 , γ_1^p , and γ_1^d are the overall surface tension and the polar and the dispersive components, respectively, of the surface tension of the liquids.

By plotting the value of $\gamma_1(1 + \cos \theta)/2(\gamma_1^d)^{0.5}$ vs. $(\gamma_1^p/\gamma_1^d)^{0.5}$, it is possible to obtain a straight line whose slope and intercept give the value of $(\gamma_S^p)^{0.5}$ and $(\gamma_S^d)^{0.5}$, respectively, for every coating surface under evaluation.

In Table III the values of γ_S , γ_S^p , and γ_S^d (obtained from the best straight lines) and the polarity parameter X_p (defined as γ_S^p/γ_S) are given for an unmodified 1 : 1 : 0.5 system and the FOTCS modified system.

In comparison with uncoated glass, the free surface energy γ_S of the coated glass with TMSM-TMOS-MMA without fluorinated precursors was lower (46.8 mJ/m² instead of 68.2 mJ/m²). The adding of small amounts of FOTCS led to a significant decrease of the polar and nonpolar part of γ_S .

Adhesion

A good level of adhesion was observed between the coatings and the glass substrate. In the base

Table IV Variation of Strength of Glasses with Hybrid Base Coating Film

Treatment	Rupture Stress (MPa)	Standard Deviation (MPa)	Percent Strengthening
Raw			
Uncoated	111	23	
+Coating	168	32	51
Abraded			
Uncoated	60	7	
+Coating	104	19	73
Indented			
Uncoated	58	6	
+Coating	114	33	96

There were 25 samples per test.

hybrid (free of fluor) no part of the coating could be removed during the adhesion test. For the fluorinated hybrid coating the amount of cross-cut area removed was less than 10%. It is important to note that the presence of fluorinated chains did not notably change the adhesion of the coating. The peel resistance was indirectly supported by the SEM observation on the hybrid-glass interface (Fig. 2). The micrograph shown in Figure 2 indicates a very good adhesion between coating and glass. In fact, fibrils usually observed in the

case of fracture of bulk hybrids are prolonged in the glass.

The good adhesion of the coating film to the glass substrate was due to the formation of Si—O—Si chemical bonds between Si—OH groups from TMOS and TMSM and the Si—OH of the glass substrate. The main advantage of the hybrid coating, in comparison with an inorganic coating produced from pure TMOS or TEOS (tetra ethoxysilane), is a more plastic behavior due to the presence of organic chains. Moreover, the presence of

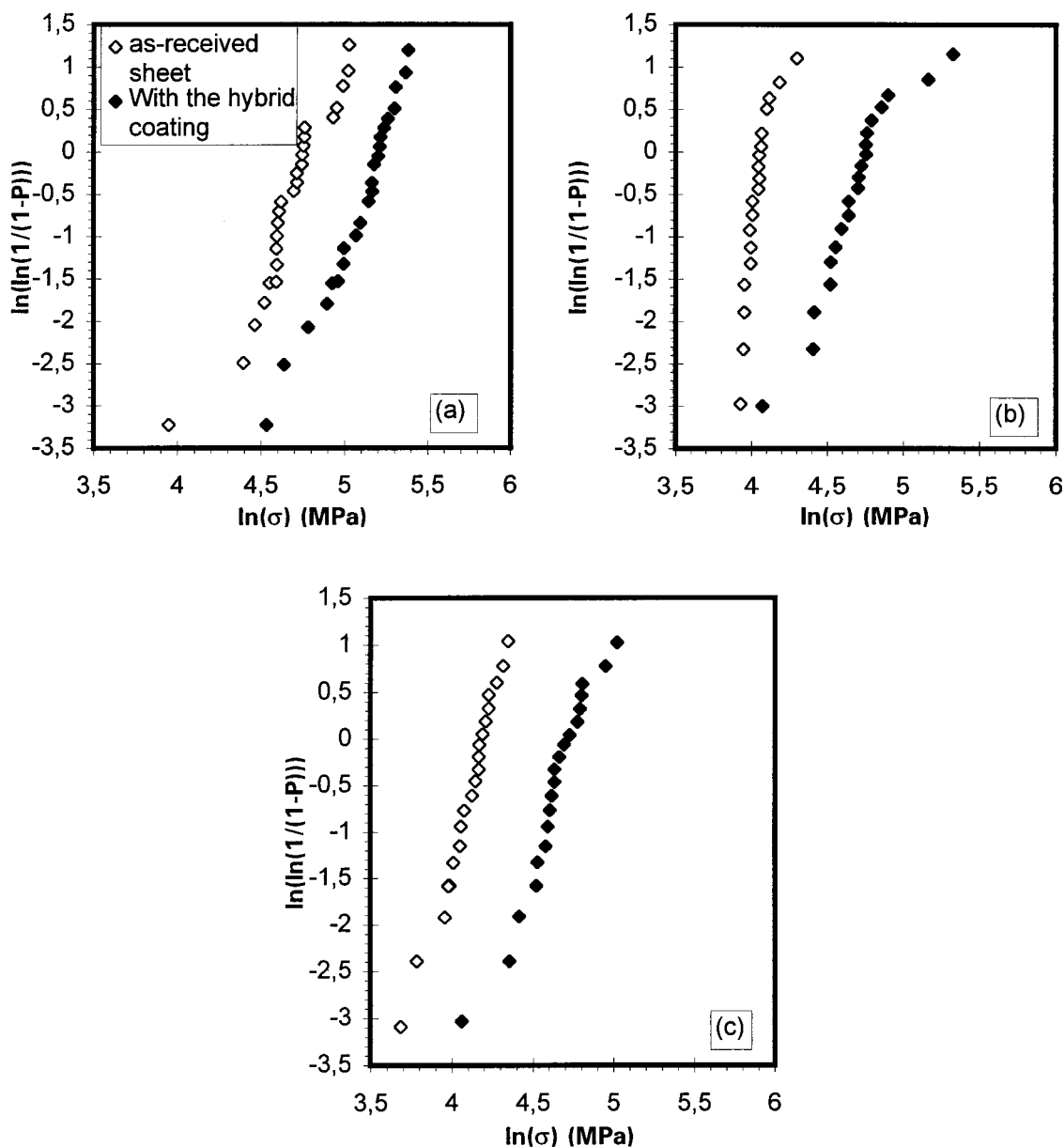


Figure 4 Weibull plots for (a) raw samples, (b) abraded samples, and (c) indented samples.

the organic phase prevents the crack formation during the drying step.

Glass Strengthening

Sol-gel coatings may improve the strength of glasses by filling in surface flaws and blunting crack tips. The Irwin theory considers the geometry of defaults by introducing the effect of the radius of a curve at the bottom of a crack³¹:

$$K_I = 1 + 2(a/\rho)^{0.5} = \sigma_1/\sigma_a$$

where σ_1 is the stress at the bottom of the crack, σ_a is the applied stress, ρ is the radius of the curve at the bottom of the crack, and a is the length of the surface flaw. All healing of the defect occurs by increasing ρ and decreasing a .

We focus on three types of defects:

1. natural defects inherent in the glass process;
2. defects artificially created by mechanical abrasion (where a is very large compared with ρ); and
3. defects created by indentation (where $a \gg \rho$); in fact, indentation leads to the formation of cracks as shown in Figure 3(a).

The experimental results are presented in Table IV. Weibull plots of the strength distributions are given in Figure 4, $\ln(\ln(1/(1-p)))$ against $\ln \sigma$, where p is the fraction of samples that failed under a tensile stress σ .^{32,33}

From Table IV and Figure 4(a) the mean strength of uncoated raw samples was increased from 111 to 168 MPa (51%). Abrasion and indentation significantly reduced the mean strength of the uncoated samples to 60 and 58 MPa, respectively. After coating, the mean strength for the abraded and the indented samples increased to 104 and 114 MPa, respectively.

This strengthening effect can be explained by the healing mechanism. There is a filling of flaws by polycondensation reaction at the surface between Si—OH bonds of the hybrid network and substrate. During coating the depth (a) decreases while the radius (ρ) increases, as shown in Figure 3(b). The relatively weak strengthening (51%) of raw glass can be explained if we consider that the initial defects during the glass making process were wide. On the other hand, for artificial defects (abrasion and indentation) the initial flaws were

narrow. The decrease in depth (a) was more important than the increase in the radius (ρ). Therefore, the strengthening effect was more important (73–96%). However, some cracks were not completely filled, and then the values obtained after coating of the raw sample were not reached.

CONCLUSION

The experimental results show that a TMSM-TMOS-MMA base hybrid system can be successfully developed to produce thin film at room temperature. The coating film has good qualities such as optical transparency, resistance to cracking, and excellent adhesion.

Hydrophobic fluorinated chains can be introduced in the hybrid system through chemical bonds, leading to an improvement of the wetting behavior without a change in the adhesion properties.

These coatings display a mechanical strengthening of the substrate that can be attributed to the filling and/or healing of the surface flaws.

REFERENCES

1. H. Scholze, *Glas, Nature, Struktur und Eigenschaften*, Springer-Verlag, Berlin, 1977.
2. A. Paul, *Chemical of Glasses*, Chapman & Hall, New York, 1990.
3. J. L. Bessede, Ph.D. dissertation, INSA, Lyon, France, 1990, p. 112.
4. J. F. Cornu, Ph.D. dissertation, INSA, Lyon, France, 1993, p. 230.
5. H. Schmidt, in *Chemical Processing of Advanced Materials*, L. L. Hench and J. K. West, Eds., Wiley, New York, 1992.
6. H. Schmidt, B. Sieferling, G. Philipp, and K. Deichmann, in *Ultrastructure of Processing of Advanced Ceramics*, J. D. Mackenzie and D. R. Ulrich, Eds., Wiley, New York, 1988, p. 651.
7. H. Schmidt, *Mater. Res. Soc. Symp. Proc.*, **171**, 3 (1990).
8. H. Schmidt, H. Scholze, and G. Tunker, *J. Non-Cryst. Solids*, **80**, 557 (1986).
9. R. Nab and H. Schmidt, in *Ceramic Powder Processing Science*, H. Hausner, G. L. Messing, and S. Hirano, Eds., Deutsche Keramische Gesellschaft, Koln, Germany, 1989, p. 69.
10. H. Krug and H. Schmidt, in *First European Workshop on Hybrid Organic-Inorganic Materials (Synthesis, Properties, Applications)*, CNRS, Chateau de Bierville, November 8–10, 1993, p. 171.

11. R. Kasemann, H. Schmidt, and S. Bruck, *Bull. Soc. Esp. Ceram.*, **7**, 75 (1992).
12. J. Kron, S. Amberg-Schwab, and G. Schottner, *J. Sol-Gel Sci. Technol.*, **2**, 189 (1994).
13. R. Kasemann and H. Schmidt, in *First European Workshop on Hybrid Organic-Inorganic Materials (Synthesis, Properties, Applications)*, CNRS, Château de Bierville, November 8-10, 1993, p. 171.
14. ASTM, *Annual Book of ASTM Standards 1990, 06.01.511*, ASTM, Philadelphia, PA, 1990.
15. J. B. Wachtman, Jr., W. Capps, and J. Mandel, *J. Mater.*, **7**, 188 (1972).
16. C. Mai, J. C. Bureau, A. Bakkali, J. F. Cornu, Z. Sassi, and F. Babonneau, in *Eurogel 92*, Strasbourg, 1992.
17. C. Mai and J. Perez, in *First European Workshop on Hybrid Organic-Inorganic Materials (Synthesis, Properties, Applications)*, CNRS, Château de Bierville, November 8-10, 1993, p. 246.
18. C. Mai, J. F. Cornu, L. Arnaud, and J. Perez, *J. Sol-Gel Sci. Technol.*, **2**, 135 (1994).
19. R. Kasemann, S. Bruck, and H. Schmidt, in *Proceedings of the 2nd European Conference on Sol-Gel Technology*, Saarbrücken, Germany, North Holland Publishers, Amsterdam, The Netherlands, 1991, p. 353.
20. C. D. Bain and G. Whitesides, *Angew. Chem.*, **101**, 522 (1989).
21. W. U. Souheng, *J. Polym. Sci. C*, **34**, 19 (1971).
22. W. U. Souheng, *J. Adhesion*, **5**, 39 (1973).
23. F. M. Fowkes, *Ind. Eng. Chem.*, **56**, 40 (1964).
24. F. M. Fowkes, *J. Phys. Chem.*, **66**, 1863 (1962).
25. D. H. Kaelble and K. C. Uy, *J. Adhesion*, **2**, 50 (1970).
26. D. K. Owens and R. C. Wendt, *J. Appl. Polym. Sci.*, **13**, 1741 (1969).
27. M. Mantel, Y. I. Rabinovich, J. P. Wightman, and R. H. Yoon, *J. Colloid Interface Sci.*, **170**, 203 (1995).
28. J. Schultz, K. Tsutumi, and J. B. Donnet, *J. Colloid Interface Sci.*, **59**, 2 (1977).
29. A. Carre and J. Schultz, *J. Adhesion*, **15**, 151 (1983).
30. W. Marconi, A. Martinelli, A. Piozzi, and D. Zane, *Macromol. Chem. Phys.*, **195**, 875 (1994).
31. R. G. Irwin, *Fracture Handbook der Physik*, Vol. 6, Springer-Verlag, Berlin, 1958, p. 551.
32. K. Trustrum and A. De S. Jayatilaka, *J. Mater. Sci.*, **18**, 2765 (1983).
33. L. Duffours, F. Pernot, T. Wolgnier, A. Alaoui, and J. Phalippou, *J. Sol-Gel Sci. Technol.*, **2**, 211 (1994).